applied sciences

MDPI

Review

A Metasurfaces Review: Definitions and Applications

Syed S. Bukhari [1], J(Yiannis) Vardaxoglou [2] and William Whittow [2,*]

[1] Department of Materials, University of Oxford, Oxford OX5 1PF, UK
[2] Wolfson School of Mechanical, Electrical and Manufacturing Engineering, Loughborough University, Loughborough LE11 3TU, UK
* Correspondence: w.g.whittow@lboro.ac.uk

Received: 30 April 2019; Accepted: 30 June 2019; Published: 5 July 2019

Abstract: This paper is a critical review of metasurfaces, which are planar metamaterials. Metamaterials offer bespoke electromagnetic applications and novel properties which are not found in naturally occurring materials. However, owing to their 3D-nature and resonant characteristics, they suffer from manufacturing complexity, losses and are highly dispersive. The 2-dimensional nature of metasurfaces allows ease of fabrication and integration into devices. The phase discontinuity across the metasurface offers anomalous refraction, thereby conserving the good metamaterial properties while still offering the low-loss characteristics. The paper discusses salient features and applications of metasurfaces; wavefront shaping; phase jumps; non-linear metasurfaces; and their use as frequency selective surfaces (FSS).

Keywords: metasurface; frequency selective surface; FSS; metamaterial; review

1. Overview

Exotic phenomena like negative refractive index and near-zero index were brought into the limelight by Pendry's work on artificial materials. These materials have their individual scatterer resonant and are generally classified as metamaterials. We start with a brief introduction to such metamaterials, however, the primary focus of this review is on their two-dimensional counterparts called metasurfaces, which are at the forefront of contemporary research. The behaviour of metamaterials and metasurfaces can be analytically explained by the expansion of Floquet modes [1]. It also needs to be mentioned that when the periodicity of these individual scatterers becomes closer in size to the wavelength of operation, higher order propagating Floquet modes need to be taken into account, to accurately describe their behaviour, such structures, therefore are not classified as metamaterials or metasurfaces [1].

2. Metamaterials

It is a widely established fact that when an electromagnetic wave strikes a composite medium, it induces electric and magnetic dipole moments in the inclusions. These dipole moments are closely related to the effective permittivity and permeability of the composite medium. Since the size, density, shape, and orientation of the inclusions can be controlled by the designer, materials with specific electromagnetic response can be synthesized. These artificially designed materials are called metamaterials. When the individual elements are resonant, such materials can possess negative values for both, relative permittivity and permeability. It needs to be emphasized that the negative refractive index is only possible with the resonant individual elements. This is due to the fact that "resonances have the characteristic that their phase response reverses as frequency changes around the resonance" [2]. Such materials are referred to in the literature as double negative media (DNG), left-handed media and backward wave media [3–5].

The electromagnetic properties of the metamaterials can be described by using the Lorentz classical theory. In this theory, the electron is treated like a damped harmonic oscillator in an electromagnetic field [6,7]. When the restoring force is negligible, the Lorentz model is reduced to the Drude model. The Drude model allows for the negative values of permittivity and permeability over a wide frequency range. Due to this property, the Drude model is sometimes preferred to than the narrowband Lorentz model for simulations [7].

Metamaterials with resonant individual elements can possess negative relative permittivity and permeability values. These left-handed materials, then according to Snell's law of refraction, make the refracted angle negative, thus causing the incident and refracted wave to lie on the same side of normal. This phenomenon is called negative refraction. Negative refraction allows the complete control of electromagnetic waves (including light), in all four quadrants of a cartesian plane. Due to this unusual characteristic, metamaterials offer potential applications which would have not been possible by only using the naturally occurring materials [7]. One of the numerous applications of the metamaterials is the phase compensation medium. DNG and positive indexed materials are combined together in such a way that the phase difference across the slab of this medium is zero. By combining double positive and double negative metamaterials, the phase difference can be controlled. It can be shown that it is the ratio of the thicknesses and the refractive index, which cause the phase difference across the medium to be zero and not the total thickness [7]. This shows that the negative index part of the slab compensates for the phase propagation in the positive index part [8]. Another interesting phenomenon which can be observed by combining the positive and negative index materials is the concentrated resonance which occurs at the interface of such two materials [9]. This interface resonance (also known as a surface wave plasmon) can replace the aperture related resonance in a traditional waveguide thus making possible the existence of sub-wavelength thin waveguides. The dispersion relation for such waveguides is also related to the thicknesses ratio and is independent of the total thickness [10,11].

Metamaterials, with a negative refractive index equal to -1, can also be used to make a superlens [12]. A superlens (also called a perfect lens) breaks the limitations imposed on focussing by wave optics (for a traditional lens, an absolute limit on the area for focussing energy, is a square of wavelength). This is due to the fact that the amplitude of the evanescent waves decays exponentially in a naturally occurring medium, whereas DNG materials enhance their amplitude. The structure still obeys the law of conservation of energy as evanescent waves do not carry any energy. It also needs to be noted that even though the refractive index is negative, the characteristic impedance (being the ratio between the permittivity and permeability) is still positive, thus there are no reflections at the interfaces, and no (mismatch) energy is lost during the whole phenomenon [12,13].

3. Metasurfaces

Metasurfaces are two-dimensional or surface counterparts of metamaterials. Just like metamaterials, it is possible to characterise their response through their electric and magnetic polarizabilities. They are also referred to in the literature as metafilms [14]. Metamaterials control the propagation of light due to their bespoke permittivity and permeability values; however, they still use the propagation effect to manipulate the electromagnetic waves. This can result in a complicated relatively bulky structure whereas metasurfaces try to manipulate the wave over a single extremely thin layer [15,16]. The two-dimensional nature of metasurfaces, therefore makes them less bulky and offers the possibility of lower loss structures [1]. Due to their 3D nature, it is also difficult to fabricate metamaterials. Metasurfaces offer an extremely promising alternative. Due to their planar structure, metasurfaces can be easily fabricated using planar fabrication tools [17,18]. The planar fabrication process is also very cost-effective in comparison to the manufacturing of the complex 3D metamaterials [19]. Metasurfaces, being two-dimensional materials, can, therefore, be easily integrated into other devices which can make them a salient feature for nanophotonic circuits; this property will also allow them to be a part of "lab on chip" photonics [20].

The negative index of the metamaterials is due to the resonance of the individual meta-atoms. This property makes the metamaterials inherently dispersive, thus the electromagnetic properties of such materials are highly sensitive to the changes in the operating frequency, thus making such materials bandwidth limited. It has been shown in [21] that by using extremely thin metasurfaces with deep sub-wavelength notches in a two-layered fishnet structure, the dispersion characteristics can be engineered. This technique was then used to make a broadband metasurface filter. The (in-band) transmission and (out of band) rejection was achieved by respectively matching and mismatching the impedance of this metasurface (to the free space). The dispersion characteristics were controlled by tailoring the primary (and secondary) magnetic resonances, and the plasma wavelengths for permittivity. Both these properties (of the metasurface) were highly dependent on the design of the sub-wavelength deep notches. The design was optimized by the help of a genetic algorithm. This broadband metasurface also had a very low insertion loss in the transmission band [21]. Due to the variety of advantages offered by metasurfaces over metamaterials, the scientific community has shown a keen recent interest in this area. This has led to rapid development in the underlying physics which govern the behaviour of metasurfaces and their potential applications.

3.1. Definition and Salient Characteristics of Metasurfaces

Metasurfaces are defined as the periodic (or aperiodic) structures where the thickness and periodicity of the individual elements (scatterers) are small in comparison to the wavelength of operation. These two-dimensional structures can be sub-classified further; an array of apertures in a reflective screen are classified as metascreens while separate individual scatterers are called metafilms [1]. However, this classification has not been usually adopted in the published literature. Metasurfaces can also be defined as a (symmetric or asymmetric) array of sub-wavelength resonant scatterers which control the electromagnetic response of the surface [16]. The distribution of individual scatterers is pivotal in determining the response of a surface. This property differentiates the metasurfaces from traditional frequency selective surfaces (FSS). A traditional FSS has individual elements (periodicity) which are of the order of the operating wavelength (generally—$\lambda/2$). Another difference between metasurfaces and FSSs is closely related to the sub-wavelength nature of the individual elements of a metasurface. The sub-wavelength nature of building blocks of metasurfaces allows them to be treated as a classic homogenous structure, thereby characterising their response with effective parameters. For a metasurface, the fields and the polarizations must be the average of the surface fields as the surface is thin. An analytical approach based on the reflection and transmission dyadic is given in [22]. Generalized sheet-transition conditions allow the complex distribution of the meta-elements to be replaced with boundary conditions by using the electric and magnetic surface susceptibilities [23]. This homogenization technique has been used to design leaky-wave antennas [24]; fractal metasurfaces [25]; and non-linear metasurfaces [26]. It is pertinent to mention that aperiodic arrangements of elements have been carried out in the design of reflect-arrays. For a reflected beam to have a specific direction, each element is designed so that it imparts the desired phase shift. Some examples are given in [27–30].

Since the response of the metasurfaces sheet is dependent on the localized behaviour of each unit, each individual unit cell is allowed to be spatially varied [16]. Such variations can be used to design metasurface lenses and shape wavefronts. The applications of the metasurfaces will be discussed in this paper. The miniaturized individual "meta-atoms" of the metasurfaces allow the sub-wavelength resolution of the wavefronts ranging from microwave to optical scale. This property of metasurfaces also allows them to behave like homogeneous or nearly homogenous sheets [31].

Another perspective to define a metasurface goes via Huygen's principle [32]. Huygen's principle states that "each point on a wavefront acts as a secondary source", thus allowing the control of wavefronts beyond the source. When an electromagnetic wave strikes a surface, it induces electric and magnetic dipole moments. These moments generate surface currents. According to Schelkunoff's principle, these surface currents are equivalent to the tangential electric and magnetic fields which control the electromagnetic response of a surface [33]. A surface can then be only characterised as

a metasurface when its every individual element is polarizable and sub-wavelength. This is achieved by careful design of the individual element(s) [31].

Metasurfaces have the ability to tailor both the electric and magnetic field component of the electromagnetic waves. Therefore, metasurfaces can have negligible mismatch losses as their impedance can be matched by tailoring the electric and magnetic polarizabilities [34,35]. Metasurfaces without reflection losses are characterised as Huygens metasurfaces [34]. In [34], two-layered metasurfaces were used to eliminate the reflection losses; the top layer was employed to temper the electric polarizability while the bottom layer was used to control the magnetic polarizability. An entirely different paradigm to structure metasurfaces is presented in [36,37]. Highly absorptive dielectrics and metals have been employed to construct a sub-wavelength thin metasurface. This metasurface achieves the desired phase shift over a nano-scale and is made with highly absorptive dielectrics and metals with finite conductivity. Since the reflection from the interface is no longer perfect, the phase can be tailored and desired phase shifts can be achieved over a much smaller distance. This is in contrast to traditional optical layers which employed extremely low loss metals and dielectrics, and exploit Fabry-Perot type interference for the phase shifts. However, unlike metasurfaces, the thickness of such (traditional) films is comparable to the operating wavelengths [37].

3.2. Phase Jumps and Generalized Law of Refraction

Conventional devices (e.g., lenses, holograms etc.) shape the wavefronts over a distance larger than the operating wavelength [38,39]. Lenses make use of their shape and the material properties (refractive index) to focus energy by gradually varying the phase of an electromagnetic wave, holograms generate images in the far-field through constructive interference [39]. The same is also true in the case of DNG materials, which also gradually temper the phase over a distance. Metasurfaces provide a promising alternative to this approach because an electromagnetic wave passing through a metasurface undergoes a phase jump. This is due to the fact that the phase is discontinuous at a metasurfaces [40]. This anomalous behaviour decreases the reliance on wave propagation and allows the shaping of wavefronts and focussing of energy over sub-wavelength distance. Therefore, metasurfaces can potentially replace the bulky and heavy devices used traditionally for such purposes.

This phase discontinuity (or jump) owes its existence to the resonant behaviour of the miniaturized (sub-wavelength) metasurface building blocks. When an electromagnetic wave strikes an individual element of a metasurface, it induces a surface electromagnetic wave. This causes the charge present in this element to oscillate. This whole phenomenon is known as surface plasmon [16]. The interaction of the impinging electromagnetic wave and the surface plasmon leads to the phase discontinuity across the metasurface. Due to this discontinuity, the Snell's law has been replaced by a "generalized law" for metasurfaces [41].

The generalized law has been derived on the basis of Fermat's principle of the least time as stationary phase [41]. Fermat's principle states that out of all the possible paths between two points, light travels on the path which takes the least amount of time [42]. Consider a plane wave at an incidence angle of θ impinging on a metasurface. Two possible paths that the wave can take are shown in Figure 1. Since the metasurface causes an abrupt change in the phase (phase discontinuity), this change at point A is shown by ϕ, while on A′ is it is represented by $\phi + d\phi$. The distance between A and A′ is assumed to be dx. It is also assumed that ϕ is a continuous function of x. It is assumed that the two paths are infinitesimally close such that the phase difference between them to reach point A is zero. This leads to the generalized refraction law given by the following Equation (1) [41].

$$n \sin(\theta) - n' \sin(\theta') = \frac{\lambda_0}{2\pi} \frac{dx}{d\phi} \tag{1}$$

where λ_0 is the free space wavelength, n and n' are the refractive indices of medium 1 and medium 2 as shown in Figure 1.

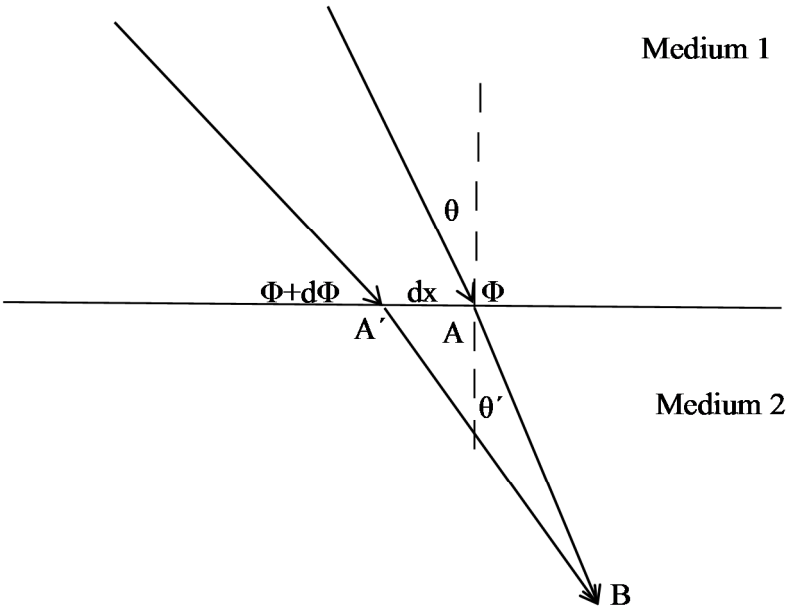

Figure 1. An illustration of generalised law of refraction. Φ and Φ + dΦ are phase discontinuities at A′ and A while dx is the distance between them. Θ′ and θ represent the angles of incidence and refraction to the normal (dotted line).

Similarly the generalised law of reflection for metasurfaces is given by Equation (2).

$$\sin(\theta) - \sin\left(\theta_{refl}\right) = \frac{\lambda_0}{2\pi n}\left|\frac{dx}{d\phi}\right| \tag{2}$$

where θ_{refl} is the angle of reflection. The non-linear relation between the incidence and the reflection is worth noting since the angle of incidence and reflection are no longer equal for a metasurface. Equations (1) and (2) can be easily reduced to the original Snell's law of refraction and reflection if there is no phase discontinuity across the surface ($d\phi/dx = 0$). The generalised laws of reflection and refraction have been demonstrated by reflectarrays and v-shaped antennas, respectively [41,43,44].

3.3. Applications of Metasurfaces

The interaction of surface plasmon with the electromagnetic wave leads to a phase discontinuity across the metasurface. Since elements on a metasurface can be spatially varied, this variation can cause the currents on the surface to lead (or lag) depending on the individual resonant element. This localized phenomenon allows us to tailor the wavefronts as they pass through a metasurface and leads to a variety of applications.

3.4. Wavefront Control/Shaping Using Metasurfaces

In the past, wavefront shaping in the microwave regime has been achieved with the help of reflect- and transmit-arrays [45,46]. Such arrays have used variable element size and rotation (in case of reflect-arrays), and aperture coupled miniaturized delay lines (with a patched ground) for the transmit-array, in order to shape the wavefronts [47,48]. Such arrays, however, have a periodicity of the order $\lambda/4 - \lambda/2$, therefore, they do not provide sub-wavelength resolution (sub-wavelength resolution can improve the aperture efficiency of such arrays) [31,49]. Due to large periodicity, the induced electric and magnetic polarizabilities can no longer completely define their response and they cannot be considered 'homogenised', hence they are not classified as metasurfaces.

Metasurfaces allow the 360° control of the phase by introducing anisotropy through its individual elements. V-shaped anisotropic elements have been used to obtain full control of the phase, however, reflection losses reduce the efficiency of the structure to 50% and since anisotropy exploits the cross-polar

component to achieve a full 360° of phase manipulation, the efficiency of the structure is further halved [16,35]. In order to unlock further potential of metasurface design, multi-layered Huygens surfaces have been proposed [50]. These surfaces eliminate the reflection losses completely. Huygen's metasurfaces with an efficiency of 86% at 10 GHz have been shown in [34]. This design also showed a wide 3-dB bandwidth of 24%.

The local phase manipulation by metasurfaces has also been used to shape the wavefronts of the reflected wave. The variation in the dimensions of square patches on a dielectric layer backed by a ground plane has been shown to tailor the reflected wavefront [51]. By carefully controlling the size and response of each sub-wavelength inclusion in along both perpendicular axes, a birefringent metasurface has been successfully constructed in [52]. This metasurface showed an efficiency of 92% with the additional advantage of splitting the incoming non-polarised electromagnetic wave into two orthogonal linear polarisations. A similar approach using perpendicular strip dipoles in a triangular lattice in terahertz range has been presented in [53]. Another technique has been developed to replicate the behaviour of arbitrary materials by using heterogeneous layers [54]. By varying the weight percentage of polyaniline micro-powder, carbon nanotubes, carbon nanofibers or graphene nanoplatelets, a series of artificial dielectrics were designed with a range of relative permittivities and loss tangents at microwave frequencies. Precise combinations of different thickness of these materials were developed via a mathematical model in conjunction with a particle swarm optimization. They were used to replicate the phase jumps of the wave going through the composite material over a frequency range. It was found that these multiple layers of artificial dielectrics could replicate the reflection coefficient of real materials, frequency selective surfaces, and even complex reflection profiles of arbitrary bespoke materials [54]. In related work, it was found that layered Cadmium iodide crystals of different sizes could be used to control the absorption over optical wavelengths [55].

3.5. Metasurface Lenses

Metasurfaces can also be employed to fabricate ultrathin lenses. In order to focus the electromagnetic energy at a distance d, a metasurface needs to have a phase profile given by Equation (3) [16].

$$\Phi_L(x, y) = \frac{2\pi}{\lambda}\left(\sqrt{x^2 + y^2 + d^2} - d\right) \tag{3}$$

This profile also alters the shape of the wavefront from planar to spherical, a condition necessary for focussing. High numerical aperture efficiency can be achieved as long as the electromagnetic wave strikes the surface at normal. However, when the angle of incidence is not perpendicular, a phenomenon known as 'coma' occurs, which can cause significant degradation in the numerical aperture efficiency. The effects of 'coma' can be reduced by placing the surface on a curved piece of dielectric [16]. Metasurface consisting of v-shaped antennas have been shown to focus energy at telecom frequencies [56]. Another metasurface lens based on reflect-arrays is presented in [57]. The lens was designed for the near infrared region and was designed on a metal-insulator-metal structure. Gold bricks were deposited on silicon dioxide and the individual elements were optimized in order to engineer the desired reflection response. This lens showed a theoretical efficiency of 78%. A metasurface lens based on rectangular dielectric resonators (RDRs) has been shown to focus energy at a single focus for three different frequencies. This was made possible by making the sum of the phase transversed by the wave and the phase jump imparted by the metasurface constant at three distinct frequencies. The resulting metasurface ended up being completely aperiodic [58].

3.6. Non-Linear Metasurfaces

Non-linear metasurfaces have been deployed to protect sensitive electronics and reduce interference on a shared platform. Non-linearity was introduced using diodes and capacitors which were incorporated in the design process and controlled the response of the metasurface. This surface absorbed the high-powered radio frequency signals while causing a minimal distortion to the low

powered ones [9]. In non-linear electrodynamics, metasurfaces and metamaterials can be used to enhance the magnitude of the non-linearity. They also allow targeting of the magnetic non-linear phenomenon and can combine it with the electric non-linearity [59]. One of the most important aspects of non-linearity is the second harmonic generation which is the process where two photons combine to form a single photon. This new photon has twice the energy and its frequency are also double in comparison to the original photon(s). This phenomenon happens when two photons interact with a non-linear material [60,61]. Metasurfaces have been deployed to enhance this process. Using fishnet metasurfaces in the near infrared region, an enhancement in the resonance of the second harmonic generation spectrum was observed using spectroscopy [61]. It needs to be noted that if a medium is inversion symmetric, it cannot generate the second harmonic and thus breaking the symmetry is imperative in order to observe the second harmonic generation.

4. Frequency Selective Surfaces Based on Metasurfaces

A typical frequency selective surface (FSS) is a periodic structure having each individual element resonant at the resonance frequency. FSSs typically have periodicity equal to half the wavelength of the resonant frequency [62]. They have been frequently employed to provide spectral filtering in signal communications. Moreover, they are also used as diplexers, beam splitters and to make antenna radomes [63]. Metasurfaces can replace FSS due to the resonant nature of "meta-atoms". Since a metasurface's building blocks are sub-wavelength in nature, they also bring additional advantages in comparison to a traditional FSS. The sub-wavelength periodicity allows to pack a large number of unit cells in a constrained space which is highly useful for radomes with limited space [64]. The small size of the unit cell also allows metasurfaces to have a stable response with respect to the changes in the angle of incidence of the illuminating electromagnetic wave. Such a structure has been presented in [65], where a layer of patches is backed by a wire grid on the other side of dielectric. The capacitance of patches coupled with the inductance of the wire grid formed an LC resonant structure with the resonant frequency much smaller than the wavelength at the resonant frequency. In addition to structural design, lumped circuit elements have also been used to miniaturize the size of a unit cell of periodic metasurfaces [66]. By using capacitors, the size of the individual element presented in [65] has been successfully decreased [67]. Convoluted elements with a reduced unit cell size have been presented in [68]. Metamaterials are usually designed with the help of split ring resonators (SRRs) [69]. SRRs have sub-wavelength physical dimensions and their Babinet's complement has been used to design and tailor the properties of metasurfaces [70]. Non-reciprocal bianisotropic elements have been used to design "one-way transparent" metasurfaces [71]. Active spatial filters (FSSs) designed using PIN and varactor diodes with complementary SRRs as their building blocks have been successfully employed for tuning and dual-band operation [72].

Once a metasurface is fabricated, its response is fixed. Its reflection and transmission response cannot be changed. However, since metasurface response is based on localized control, reconfigurable metasurfaces are very much desired in order to use a single metasurface for a wide range of applications. This has been addressed by a variety of designs presenting tuneable/reconfigurable metasurfaces. There are three major ways in which a metasurface can be tuned (i) mechanical tuning (ii) material state change under a stimulus (iii) use of varactor diodes (in microwave domain) [73]. Mechanical tuning in all dielectric metasurfaces has been used in [74] and a shift in both resonances was recorded by rotating the individual elements. MEMS have also been applied for mechanical tuning in [75]. By shifting an engineered ground plane, beam steering from a reflector has also been achieved [76]. The capacitance of varactor diodes can be controlled by varying the voltage across them which make them an excellent candidate for electrically tuning the metasurfaces [77]. These diodes have been used for beam steering and switching the states(modes) of metasurfaces [78,79]. A tuneable metasurface with 1125 varactor diodes in a planar array has used as a steerable reflector [78]. Metasurfaces with dispersive refractive index have been proposed for THz domain since the modulators at THz frequency usually work at extremely low (cryogenic) temperatures [80].

The use of multilayers to improve the response of an FSS has been well documented [62]. Multi-layered FSSs, formed by cascading two or more layers of the periodic structures and carefully aligning them, has led to an increase in the operational bandwidth of the structure and improve the filter's roll-off rate, thus making them available to be used for de-multiplexing in multiband radiometers [81]. Multi-layered structures have also been demonstrated to reduce the size of the individual elements of FSSs, an inductive grid of wires fabricated on one side of the substrate with the other side having a loop grid in which every element is connected to its neighbours with a capacitor. This structure showed a relatively stable frequency response to the changes in the angle of incidence [82]. A multi-layered square patch complementary structure has been utilized to improve the gain of an antenna over a wide bandwidth by using Fabry-Perrot resonance [83]. Multi-layered periodic structures designed using a genetic algorithm have been used to construct an artificial magnetic conductor [84]. A similar approach has also been employed in the area of metasurfaces. A three-layered efficient metasurface for controlling the phase and magnitude of the transmitting beam using horizontally and vertically aligned split-rings has been presented in [85].

5. Metasurface Antennas

Metasurfaces have been successfully used to design and manufacture high gain holographic antennas [86,87]. For holographic antennas, the surface wave is the major incident wave. The radiation for such antennas occurs when phase matching between forward and backward leaky wave occurs. Forward leaky wave arises from the grating which has a larger periodicity while the smaller period grating leads to a backward leaky wave. A source with elliptic grating is surrounded by both periodicities. Both leaky wave modes for such a grating are matched leading to directive radiation [88]. Based on this approach, circularly polarized leaky wave antennas with a 26 dB gain are presented in [86]. The grating effect was produced by modulating the surface impedance of the metasurface. A significant advantage of this approach is that instead of changing the antenna shape in order to design a specific response, the metasurface modulation (i.e., surface impedance) is engineered [89]. A metasurface antenna offering the possibility of both right- and left-hand circular polarization was presented in [90]. Both TE and TM surface waves were launched and the polarization decoupling of the two modes was utilized for their independent control. These modes were phase-matched and the modulated metasurface was rotationally symmetric. The antenna was fed by a circular waveguide and a corrugated hat was placed on top of the waveguide to suppress the space-wave radiation. Since phase-matching is critical for leaky-wave metasurface antennas, a bandwidth of such antennas is limited by the dispersion of the metasurface. The mismatch of phase leads to a decrease in the gain of structure. A bandwidth gain expression for these antennas is available in [91]. It was shown that this bandwidth can be increased by designing the modulated metasurface on a low permittivity dielectric and increasing the antenna size. It has also been shown that metasurface antennas can be designed for multi-beam operation [92]. Another use of metasurfaces for leaky wave antennas are Non-chiral bianisotropic metasurfaces called omega metasurfaces. When periodic leaky wave antennas are used to scan the broadside, Floquet mode coupling deteriorates its radiation performance. Non-chiral bianisotropic metasurfaces can be employed to solve this problem. Moreover, it has been discovered that metasurfaces of any period can be used to design such leaky wave antennas. There is no issue of Floquet mode coupling since only a single mode is excited [93]. The use of multi-layered Huygen's metasurfaces to structure a bianisotropic metasurface has been proposed in [94].

In [95], multi-layered metasurfaces with sub-wavelength profile were used as partial reflective surfaces to design a high gain antenna with an enhanced bandwidth. In [96], Huygen's metasurfaces have been proposed to convert a non-directive beam from an arbitrary source to a directive one. Such metasurfaces have been utilised to construct a low profile antenna with high aperture efficiency by employing them as a partially reflective surface fed by a cavity [97]. The aid of Babinet's principle can be used to develop complementary metasurfaces. A comprehensive treatment of such metasurface design with an equivalent circuit has been presented in [98]. The complementary metasurfaces have

been used to design antennas and transmission lines, and offer the possibility of tuneable antennas and circuits [99]. Metasurfaces can also improve the performance of horn antennas. In [100], a metasurface designed using a genetic algorithm has been used as an inner surface for a conical horn and the cross polar levels and the side lobe levels have been improved over the entire Ku band. A similar approach was applied to improve the performance of a hybrid mode square horn antenna using metasurfaces [101]. Metasurfaces have been proposed for medical body area networks (MBAN) as well, by improving the performance of a low-profile monopole antenna. The truncated metasurface, in contrast to artificial magnetic conductors (AMCs), also contributed to the radiation from the antenna thus increasing the gain and the front to back ratio [102]. Two-layered metasurfaces loaded with resistors have been demonstrated to reduce the radar cross section (RCS) of a stacked antenna array thus offering an alternative to radar absorbing material. The antenna was sandwiched between these two metasurfaces, the metafilm above the antenna reduced the RCS for out of band frequencies while the one below reduced the RCS for the in-band frequencies [103].

6. Summary

The purpose of this review paper has been to state a comprehensive suitable definition of a metasurface and identify its salient features as well as highlight some of the numerous advantages which can be achieved through the use of metasurfaces. The sub-wavelength nature of building blocks of metasurfaces allows them to be defined using homogeneous boundary conditions. Another important characteristic of metasurfaces is the phase discontinuity which occurs when an electromagnetic wave goes through a metasurface. Both these behaviours can be successfully described by using generalised refraction and reflection laws. A superior feature of metasurfaces is its low-loss behaviour (as demonstrated particularly by Huygen's metasurfaces) in stark contrast to metamaterials. Thus, metasurfaces allow us to utilise the exotic properties of metamaterials like engineered refraction and reflection without inducing manufacturing complexity and losses associated with metamaterials. Metasurfaces also offer spatial filters with a stable frequency response with respect to the incidence angle.

Although considerable successful work has been done on metasurfaces in the microwave regime, the inclusion of metasurfaces in the design for future communication and imaging devices is still an area with immense potential for research and growth. Bandwidth is a non-negotiable key requirement for most RF applications therefore, future challenges will include designing metasurfaces with a stable phase and frequency response over a wide band. Another important aspect would be switch-able or active metasurfaces which are cost-effective and relatively simple to fabricate. The addition of switching components can introduce non-linearities in the metasurface which would merit a sound theoretical investigation.

Author Contributions: The lead author of this paper is S.S.B. Additional support was provided by W.W. and Y.V.

Funding: This research was funded by EPSRC, grant number EP/S030301/1, "Anisotropic Microwave/Terahertz Metamaterials for Satellite Applications (ANISAT)".

Conflicts of Interest: The authors declare no conflict of interest.

References

1. Holloway, C.L.; Kuester, E.F.; Gordon, J.A.; O'Hara, J.; Booth, J.; Smith, D.R. An Overview of the Theory and Applications of Metasurfaces: The Two-Dimensional Equivalents of Metamaterials. *IEEE Antennas Propag. Mag.* **2012**, *54*, 10–35. [CrossRef]
2. Pendry, J.B. Metamaterials and the Control of Electromagnetic Fields. In Proceedings of the Conference on Coherence and Quantum Optics 2007, Rochester, NY, USA, 10–13 June 2007; pp. 1–11.
3. Caloz, C.; Okabe, H.; Iwai, T.; Itoh, T. Transmission line approach of left-handed materials. In Proceedings of the IEEE AP-S International Symposium and USNC/URSINational Radio Science Meeting, San Antonio, TX, USA, 16 June 2002; p. 39.

4. Lindell, I.V.; Tretyakov, S.A.; Nikoskinen, K.I.; Ilvonen, S. BW media? Media with negative parameters, capable of supporting backward waves. *Microw. Opt. Technol. Lett.* **2001**, *31*, 129–133. [CrossRef]
5. Ziolkowski, R.W.; Heyman, E. Wave propagation in media having negative permittivity and permeability. *Phys. Rev. E* **2001**, *64*, 056625. [CrossRef] [PubMed]
6. Lorentz, T. Lorentz Dispersion Model. 1878. Available online: http://www.horiba.com/fileadmin/uploads/Scientific/Downloads/OpticalSchool_CN/TN/ellipsometer/Lorentz_Dispersion_Model.pdf (accessed on 13 February 2019).
7. Engheta, N.; Ziolkowski, R. *Metamaterials: Physics and Engineering Explaorations*; Wiley-IEEE Press: Piscataway, NJ, USA, 2006.
8. Engheta, N. Ideas for potential applications of metamaterials with negative permittivity and permeability. In *Advances in Electromagnetics of Complex Media and Metamaterials*; Springer: Dordrecht, The Netherlands, 2002.
9. Engheta, N. An Idea for Thin Subwavelength Cavity Resonators Using Metamaterials with Negative Permittivity and Permeability. *IEEE Antennas Wirel. Propag. Lett.* **2002**, *1*, 10–13. [CrossRef]
10. Engheta, N.; Ziolkowski, R.W. A positive future for double-negative metamaterials. *IEEE Trans. Microw. Theory Tech.* **2005**, *53*, 1535–1556. [CrossRef]
11. Alù, A.; Engheta, N. Guided Modes in a Waveguide Filled with a Pair of SNG, DNG and/or DPS Layers. *IEEE Trans. Microw. Theory Tech.* **2004**, *52*, 199–210. [CrossRef]
12. Pendry, J.B. Negative Refraction Makes a Perfect Lens. *Phys. Rev. Lett.* **2000**, *85*, 3966–3969. [CrossRef]
13. Veselago, V.G. The Electrodynamics of substances with simultaneously negative values of ϵ and μ. *Phys. Uspekhi* **1968**, *10*, 509–514. [CrossRef]
14. Kuester, E.; Mohamed, M.; Piket-May, M.; Holloway, C. Averaged transition conditions for electromagnetic fields at a metafilm. *IEEE Trans. Antennas Propag.* **2003**, *51*, 2641–2651. [CrossRef]
15. Cai, W.; Shalaev, V.M. *Optical Metamaterials: Fundamentals and Applications*; Springer: Berlin, Germany, 2009.
16. Yu, N.; Capasso, F. Flat optics with designer metasurfaces. *Nat. Mater.* **2014**, *13*, 139–150. [CrossRef]
17. Yoon, G.; Kim, I.; Rho, J. Microelectronic engineering challenges in fabrication towards realization of practical metamaterials. *Microelectron. Eng.* **2016**, *163*, 7–20. [CrossRef]
18. Soukoulis, C.M.; Wegener, M. Past achievements and future challenges in the development of three-dimensional photonic metamaterials. *Nat. Photonics* **2011**, *5*, 523–530. [CrossRef]
19. Meinzer, N.; Barnes, W.L.; Hooper, I.R. Plasmonic meta-atoms and metasurfaces. *Nat. Photon.* **2014**, *8*, 889–898. [CrossRef]
20. Kildishev, A.V.; Boltasseva, A.; Shalaev, V.M. Planar Photonics with Metasurfaces. *Science* **2013**, *339*, 1232009. [CrossRef] [PubMed]
21. Jiang, Z.H.; Yun, S.; Lin, L.; Bossard, J.A.; Werner, D.H.; Mayer, T.S. Tailoring Dispersion for Broadband Low-loss Optical Metamaterials Using Deep-subwavelength Inclusions. *Sci. Rep.* **2013**, *3*, 1571. [CrossRef] [PubMed]
22. Albooyeh, M.; Simovski, C.; Tretyakov, S. Homogenization and characterization of metasurfaces: General framework. In Proceedings of the 2016 10th European Conference on Antennas and Propagation (EuCAP), Davos, Switzerland, 10–15 April 2016; pp. 1–3.
23. Holloway, C.L.; Kuester, E.F. A Homogenization Technique for Obtaining Generalized Sheet-Transition Conditions for a Metafilm Embedded in a Magnetodielectric Interface. *IEEE Trans. Antennas Propag.* **2016**, *64*, 4671–4686. [CrossRef]
24. Fuscaldo, W.; Tofani, S.; Zografopoulos, D.C.; Baccarelli, P.; Burghignoli, P.; Beccherelli, R.; Galli, A. Systematic Design of THz Leaky-Wave Antennas Based on Homogenized Metasurfaces. *IEEE Trans. Antennas Propag.* **2018**, *66*, 1169–1178. [CrossRef]
25. Moeini, S. Homogenization of Fractal Metasurface Based on Extension of Babinet-Booker's Principle. *IEEE Antennas Wirel. Propag. Lett.* **2019**, *18*, 1061–1065. [CrossRef]
26. Achouri, K.; Bernasconi, G.D.; Butet, J.; Martin, O.J.F. Homogenization and Scattering Analysis of Second-Order Nonlinear Metasurfaces. In Proceedings of the 2018 12th International Congress on Artificial Materials for Novel Wave Phenomena (Metamaterials), Espoo, Finland, 27 August–1 September 2018; Volume 66, pp. 10–12.
27. Carrasco, E.; Encinar, J.A. Reflectarray antennas: A review. *Forum Electromagn. Res. Methods Appl. Technol.* **2016**.
28. Cho, Y.H.; Byun, W.J.; Song, M.S. Metallic-Rectangular-Grooves Based 2D Reflectarray Antenna Excited by an Open-Ended Parallel-Plate Waveguide. *IEEE Trans. Antennas Propag.* **2010**, *58*, 1788–1792.

29. Encinar, J.; Zornoza, J. Broadband design of three-layer printed reflectarrays. *IEEE Trans. Antennas Propag.* **2003**, *51*, 1662–1664. [CrossRef]
30. Huang, J.; Pogorzelski, R. A Ka-band microstrip reflectarray with elements having variable rotation angles. *IEEE Trans. Antennas Propag.* **1998**, *46*, 650–656. [CrossRef]
31. Glybovski, S.B.; Tretyakov, S.A.; Belov, P.A.; Kivshar, Y.S.; Simovski, C.R. Metasurfaces: From microwaves to visible. *Phys. Rep.* **2016**, *634*, 1–72. [CrossRef]
32. Huygens, C. *Traite' de la Lumie're (A Treatise on light)*; Pieter van der Aa: Leyden, The Netherlands, 1690.
33. Rengarajan, S.; Rahmat-Samii, Y. The field equivalence principle: Illustration of the establishment of the non-intuitive null fields. *IEEE Antennas Propag. Mag.* **2000**, *42*, 122–128. [CrossRef]
34. Pfeiffer, C.; Grbic, A. Metamaterial Huygens' surfaces: Tailoring wave fronts with reflectionless sheets. *Phys. Rev. Lett.* **2013**, *110*, 1–5. [CrossRef] [PubMed]
35. Monticone, F.; Estakhri, N.M.; Alù, A. Full Control of Nanoscale Optical Transmission with a Composite Metascreen. *Phys. Rev. Lett.* **2013**, *110*, 1–5. [CrossRef] [PubMed]
36. Kats, M.A.; Sharma, D.; Lin, J.; Genevet, P.; Blanchard, R.; Yang, Z.; Qazilbash, M.M.; Basov, D.N.; Ramanathan, S.; Capasso, F. Ultra-thin perfect absorber employing a tunable phase change material. *Appl. Phys. Lett.* **2012**, *101*, 221101. [CrossRef]
37. Kats, M.A.; Blanchard, R.; Genevet, P.; Capasso, F. Nanometre optical coatings based on strong interference effects in highly absorbing media. *Nat. Mater.* **2012**, *12*, 20–24. [CrossRef] [PubMed]
38. Cornbleet, S. Geometrical Optics Reviewed: A new light on an old subject. *Proc. IEEE* **1983**, *71*, 471–502. [CrossRef]
39. Cathey, J.W. Three-Dimensional Wavefront Reconstruction Using a Phase Hologram. *J. Opt. Soc. Am.* **1965**, *1295*, 457. [CrossRef]
40. Zhang, Y.; Liang, L.; Yang, J.; Feng, Y.; Zhu, B.; Zhao, J.; Jiang, T.; Jin, B.; Liu, W. Broadband diffuse terahertz wave scattering by flexible metasurface with randomized phase distribution. *Sci. Rep.* **2016**, *6*, 26875. [CrossRef] [PubMed]
41. Yu, N.; Genevet, P.; Kats, M.A.; Aieta, F.; Tetienne, J.-P.; Capasso, F.; Gaburro, Z. Light Propagation with Phase Discontinuities: Generalized Laws of Reflection and Refraction. *Science* **2011**, *334*, 333–337. [CrossRef] [PubMed]
42. Feynman, R.; Leighton, R.; Sands, M. The Feynman lectrures on physics I. *Am. J. Phys.* **1965**, *33*, 750–752. [CrossRef]
43. Ni, X.; Emani, N.K.; Kildishev, A.V.; Boltasseva, A.; Shalaev, V.M. Broadband Light Bending with Plasmonic Nanoantennas. *Science* **2012**, *335*, 427. [CrossRef] [PubMed]
44. Yu, N.; Aieta, F.; Genevet, P.; Kats, M.A.; Gaburro, Z.; Capasso, F. A Broadband, Background-Free Quarter-Wave Plate Based on Plasmonic Metasurfaces. *Nano Lett.* **2012**, *12*, 6328–6333. [CrossRef] [PubMed]
45. Mcgrath, D.T. Planar Three-Dimensional Constrained Lenses. *IEEE Trans. Antennas Propag.* **1986**, *34*, 46–50. [CrossRef]
46. Pozar, D.M.; Targonski, S.D.; Syrigos, H.D. Design of millimeter wave microstrip reflectarrays. *IEEE Trans. Antennas Propag.* **1997**, *45*, 287–296. [CrossRef]
47. Yu, A.; Yang, F.; Elsherbeni, A.; Huang, J. Experimental demonstration of a single layer tri-band circularly polarized reflectarray. In Proceedings of the 2010 IEEE Antennas and Propagation Society International Symposium, Toronto, ON, Canada, 11–17 July 2010; pp. 1–4.
48. Pozar, D.M. Flat lens antenna concept using aperture coupled microstrip patches. *Electron. Lett.* **1996**, *32*, 2109–2111. [CrossRef]
49. Pozar, D.M. Wideband reflectarrays using artificial impedance surfaces. *Electron. Lett.* **2007**, *43*, 148. [CrossRef]
50. Niemi, T.; Karilainen, A.O.; Tretyakov, S.A. Synthesis of Polarization Transformers. *IEEE Trans. Antennas Propag.* **2013**, *61*, 3102–3111. [CrossRef]
51. Ginn, J.; Lail, B.; Alda, J.; Boreman, G. Planar infrared binary phase reflectarray. *Opt. Lett.* **2008**, *33*, 779–781. [CrossRef] [PubMed]
52. Farmahini-Farahani, M.; Mosallaei, H. Birefringent reflectarray metasurface for beam engineering in infrared. *Opt. Lett.* **2013**, *38*, 462–464. [CrossRef] [PubMed]
53. Niu, T.; Withayachumnankul, W.; Upadhyay, A.; Gutruf, P.; Abbott, D.; Bhaskaran, M.; Sriram, S.; Fumeaux, C. Terahertz reflectarray as a polarizing beam splitter. *Opt. Express* **2014**, *22*, 16148–16160. [CrossRef] [PubMed]

54. Micheli, D.; Pastore, R.; Vricella, A.; Marchetti, M. Matter's Electromagnetic Signature Reproduction by Graded-Dielectric Multilayer Assembly. *IEEE Trans. Microw. Theory Tech.* **2017**, *65*, 2801–2809. [CrossRef]
55. Bellucci, S.; Bolesta, I.; Guidi, M.C.; Karbovnyk, I.; Lesivciv, V.; Micciulla, F.; Pastore, R.; Popov, A.I.; Velgosh, S. Cadmium clusters in CdI2layered crystals: The influence on the optical properties. *J. Phys. Condens. Matter* **2007**, *19*, 395015. [CrossRef]
56. Aieta, F.; Genevet, P.; Kats, M.A.; Yu, N.; Blanchard, R.; Gaburro, Z.; Capasso, F. Aberration-Free Ultrathin Flat Lenses and Axicons at Telecom Wavelengths Based on Plasmonic Metasurfaces. *Nano Lett.* **2012**, *12*, 4932–4936. [CrossRef] [PubMed]
57. Pors, A.; Nielsen, M.G.; Eriksen, R.L.; Bozhevolnyi, S.I. Broadband Focusing Flat Mirrors Based on Plasmonic Gradient Metasurfaces. *Nano Lett.* **2013**, *13*, 829–834. [CrossRef]
58. Aieta, F.; Kats, M.A.; Genevet, P.; Capasso, F. Multiwavelength achromatic metasurfaces by dispersive phase compensation. *Science* **2015**, *347*, 1342–1345. [CrossRef]
59. Lapine, M.; Shadrivov, I.V.; Kivshar, Y.S. Colloquium: Nonlinear metamaterials. *Rev. Mod. Phys.* **2014**, *86*, 1093–1123. [CrossRef]
60. Wang, Z.; Chen, J.; Wu, Z.; Zhu, Y. Wave propagation in two-dimensional left-handed non-linear transmission line metamaterials. *IET Microw. Antennas Propag.* **2016**, *10*, 202–207. [CrossRef]
61. Kim, E.; Wang, F.; Wu, W.; Yu, Z.; Shen, Y.R. Nonlinear optical spectroscopy of photonic metamaterials. *Phys. Rev. B* **2008**, *78*, 2–5. [CrossRef]
62. Vardaxoglou, J.C. *Frequency Selective Surfaces: Analysis and Design*; Research Studies Press: Boston, MA, USA, 1997.
63. Lee, S.-W. Scattering by dielectric-loaded screen. *IRE Trans. Antennas Propag.* **1971**, *19*, 656–665.
64. Chiu, C.-N.; Chang, K.-P. A Novel Miniaturized-Element Frequency Selective Surface Having a Stable Resonance. *IEEE Antennas Wirel. Propag. Lett.* **2009**, *8*, 1175–1177. [CrossRef]
65. Sarabandi, K.; Behdad, N. A Frequency Selective Surface with Miniaturized Elements. *IEEE Trans. Antennas Propag.* **2007**, *55*, 1239–1245. [CrossRef]
66. Xu, R.-R.; Zong, Z.-Y.; Wu, W. Low-frequency miniaturized dual-band frequency selective surfaces with close band spacing. *Microw. Opt. Technol. Lett.* **2009**, *51*, 1238–1240. [CrossRef]
67. Bayatpur, F.; Sarabandi, K. A Tunable Metamaterial Frequency-Selective Surface with Variable Modes of Operation. *IEEE Trans. Microw. Theory Tech.* **2009**, *57*, 1433–1438. [CrossRef]
68. Sanz-Izquierdo, B.; Parker, E.A.; Robertson, J.-B.; Batchelor, J.C. Singly and Dual Polarized Convoluted Frequency Selective Structures. *IEEE Trans. Antennas Propag.* **2010**, *58*, 690–696. [CrossRef]
69. Pendry, J.; Holden, A.; Robbins, D.; Stewart, W. Magnetism from conductors and enhanced nonlinear phenomena. *IEEE Trans. Microw. Theory Tech.* **1999**, *47*, 2075–2084. [CrossRef]
70. Falcone, F.; Lopetegi, T.; Laso, M.A.G.; Baena, J.D.; Bonache, J.; Beruete, M.; Marques, R.; Martin, F.; Sorolla, M. Babinet Principle Applied to the Design of Metasurfaces and Metamaterials. *Phys. Rev. Lett.* **2004**, *93*, 197401. [CrossRef]
71. Ra, Y.; Asadchy, V.S.; Tretyakov, S.A. One-way transparent sheets. *Phys. Rev. B* **2014**, *89*, 075109.
72. Sanz-Izquierdo, B.; Parker, E.A.; Batchelor, J. Dual-Band Tunable Screen Using Complementary Split Ring Resonators. *IEEE Trans. Antennas Propag.* **2010**, *58*, 3761–3765. [CrossRef]
73. Turpin, J.P.; Bossard, J.A.; Morgan, K.L.; Werner, D.H.; Werner, P.L. Reconfigurable and Tunable Metamaterials: A Review of the Theory and Applications. *Int. J. Antennas Propag.* **2014**, *2014*, 429837. [CrossRef]
74. Li, L.; Wang, J.; Wang, J.; Ma, H.; Du, H.; Zhang, J.; Qu, S.; Xu, Z. Reconfigurable all-dielectric metamaterial frequency selective surface based on high-permittivity ceramics. *Sci. Rep.* **2016**, *6*, 24178. [CrossRef] [PubMed]
75. Debogovi, T.; Bartolic, J.; Perruisseau-Carrier, J. Dual-Polarized Partially Refl ective Surface Antenna with MEMS-Based Beamwidth Reconfiguratio. *IEEE Trans. Antennas Propag.* **2014**, *62*, 228–236. [CrossRef]
76. Sievenpiper, D.; Schaffner, J.; Tangonan, G.; Ontiveros, S.; Harold, R.; Loo, R. A tunable impedance surface performing as a reconfigurable beam steering reflector. *IEEE Trans. Antennas Propag.* **2002**, *50*, 384–390. [CrossRef]
77. Bakanowski, A.E.; Cranna, N.G.; Uhlir, J.A. Diffused Silicon Nonlinear Capacitors. *IRE Trans. Electron Devices* **1958**, *17*, 384–390.
78. Sievenpiper, D.F.; Schaffner, J.H.; Song, H.J.; Loo, R.Y.; Tangonan, G. Two-Dimensional Beam Steering Using an Electrically Tunable Impedance Surface. *IEEE Trans. Antennas Propag.* **2003**, *51*, 2713–2722. [CrossRef]

79. Bayatpur, F.; Sarabandi, K. Design and Analysis of a Tunable Miniaturized-Element Frequency-Selective Surface Without Bias Network. *IEEE Trans. Antennas Propag.* **2010**, *58*, 1214–1219. [CrossRef]
80. Chen, H.-T.; Padilla, W.J.; Zide, J.M.O.; Gossard, A.C.; Taylor, A.J.; Averitt, R.D. Active terahertz metamaterial devices. *Nature* **2006**, *444*, 597–600. [CrossRef]
81. Antonopoulos, C.; Cahill, R.; Parker, E.; Sturland, I. Multilayer frequency-selective surfaces for millimetre and submillimetre wave applications. *IEE Proc. Microw. Antennas Propag.* **1997**, *144*, 415. [CrossRef]
82. Bayatpur, F.; Sarabandi, K. Single-Layer High-Order Miniaturized-Element. *IEEE Trans. Microw. Theory Tech.* **2008**, *56*, 774–781. [CrossRef]
83. Wang, N.; Liu, Q.; Wu, C.; Talbi, L. Wideband Fabry-Perot Resonator Antenna With Two Complementary FSS Layers. *IEEE Trans. Antennas Propag.* **2014**, *62*, 2463–2471.
84. Monorchio, A.; Manara, G.; Lanuzza, L. Synthesis of artificial magnetic conductors by using multilayered frequency selective surfaces. *IEEE Antennas Wirel. Propag. Lett.* **2002**, *1*, 196–199. [CrossRef]
85. Wan, X.; Jia, S.L.; Cui, T.J.; Zhao, Y.J. Independent modulations of the transmission amplitudes and phases by using Huygens metasurfaces. *Sci. Rep.* **2016**, *6*, 25639. [CrossRef] [PubMed]
86. Minatti, G.; Caminita, F.; Casaletti, M.; Maci, S. Spiral leaky-wave antennas based on modulated surface impedance. *IEEE Trans. Antennas Propag.* **2011**, *59*, 4436–4444. [CrossRef]
87. Gregoire, D.J. 3-D Conformal Metasurfaces. *IEEE Antennas Wirel. Propag. Lett.* **2013**, *12*, 233–236. [CrossRef]
88. Nannetti, M.; Caminita, F.; Maci, S. Leaky-wave based interpretation of the radiation from holographic surfaces. In Proceedings of the 2007 IEEE Antennas and Propagation Society International Symposium, Honolulu, HI, USA, 9–15 June 2007; pp. 5813–5816.
89. Minatti, G.; Faenzi, M.; Martini, E.; Caminita, F.; De Vita, P.; Ovejero, D.G.; Sabbadini, M.; Maci, S. Modulated Metasurface Antennas for Space: Synthesis, Analysis and Realizations. *IEEE Trans. Antennas Propag.* **2015**, *63*, 1288–1300. [CrossRef]
90. Pereda, A.T.; Caminita, F.; Martini, E.; Ederra, I.; Iriarte, J.C.; Gonzalo, R.; Maci, S.; Tellechea, A. Dual Circularly-Polarized Broadside Beam Metasurface Antenna. *IEEE Trans. Antennas Propag.* **2016**, *64*, 2944–2953. [CrossRef]
91. Minatti, G.; Faenzi, M.; Sabbadini, M.; Maci, S. Bandwidth of Gain in Metasurface Antennas. *IEEE Trans. Antennas Propag.* **2017**, *65*, 2836–2842. [CrossRef]
92. González-ovejero, D.; Member, S.; Minatti, G.; Chattopadhyay, G.; Maci, S. Multibeam by Metasurface Antennas. *IEEE Trans. Antennas Propag.* **2017**, *65*, 2923–2930. [CrossRef]
93. Abdo-Sanchez, E.; Chen, M.; Epstein, A.; Eleftheriades, G.V. A Leaky-Wave Antenna with Controlled Radiation Using a Bianisotropic Huygens' Metasurface. *IEEE Trans. Antennas Propag.* **2019**, *67*, 108–120. [CrossRef]
94. Epstein, A.; Eleftheriades, G.V. Arbitrary Power-Conserving Field Transformations with Passive Lossless Omega-Type Bianisotropic Metasurfaces. *IEEE Trans. Antennas Propag.* **2016**, *64*, 3880–3895. [CrossRef]
95. Konstantinidis, K.; Feresidis, A.P.; Hall, P.S. Broadband Sub-Wavelength Profile High-Gain Antennas Based on Multi-Layer Metasurfaces. *IEEE Trans. Antennas Propag.* **2015**, *63*, 423–427. [CrossRef]
96. Epstein, A.; Eleftheriades, G.V. Passive Lossless Huygens Metasurfaces for Conversion of Arbitrary Source Field to Directive Radiation. *IEEE Trans. Antennas Propag.* **2014**, *62*, 5680–5695. [CrossRef]
97. Epstein, A.; Wong, J.P.S.; Eleftheriades, G.V. Cavity-excited Huygens' metasurface antennas for near-unity aperture illumination efficiency from arbitrarily large apertures. *Nat. Commun.* **2016**, *7*, 1–10. [CrossRef] [PubMed]
98. Bukhari, S.S.; Whittow, W.G.; Vardaxoglou, J.C.; Maci, S.; Whittow, W.; Vardaxoglou, J.Y. Equivalent Circuit Model for Coupled Complementary Metasurfaces. *IEEE Trans. Antennas Propag.* **2018**, *66*, 5308–5317. [CrossRef]
99. Ovejero, D.G.; Martini, E.; Loiseaux, B.; Tripon-Canseliet, C.; Mencagli, M.J.; Chazelas, J.; Maci, S. Basic Properties of Checkerboard Metasurfaces. *IEEE Antennas Wirel. Propag. Lett.* **2015**, *14*, 406–409. [CrossRef]
100. Wu, Q.; Scarborough, C.P.; Werner, D.H.; Lier, E.; Wang, X. Design Synthesis of Metasurfaces for Broadband Hybrid-Mode Horn Antennas with Enhanced Radiation Pattern and Polarization Characteristics. *IEEE Trans. Antennas Propag.* **2012**, *60*, 3594–3604. [CrossRef]
101. Scarborough, C.P.; Martin, B.G.; Shaw, R.K.; Werner, D.H.; Lier, E.; Wang, X.; Wu, Q. A *Ku*-Band Dual Polarization Hybrid-Mode Horn Antenna Enabled by Printed-Circuit-Board Metasurfaces. *IEEE Trans. Antennas Propag.* **2013**, *61*, 1089–1098.

102. Jiang, Z.H.; Brocker, D.E.; Sieber, P.E.; Werner, D.H. A Compact, Low-Profile Metasurface-Enabled Network Devices. *IEEE Trans. Antennas Propag.* **2014**, *62*, 4021–4030. [CrossRef]
103. Huang, C.; Pan, W.; Ma, X.; Luo, X. Wideband Radar Cross Section Reduction of a Stacked Patch Array Antenna Using Metasurface. *IEEE Antennas Wirel. Propag. Lett.* **2015**, *14*, 1369–1372. [CrossRef]